SANDIA REPORT
SAND97-2214 • UC-701
Unlimited Release
Printed September 1997

Ultra-High-Speed Studies of Shock Phenomena in a Miniaturized System: A Preliminary Evaluation

Wayne M. Trott, Kenneth L. Erickson

Prepared by
Sandia National Laboratories
Albuquerque, New Mexico 87185 and Livermore, California 94550

Sandia is a multiprogram laboratory operated by Sandia Corporation, a Lockheed Martin Company, for the United States Department of Energy under Contract DE-AC04-94AL85000.

Sandia National Laboratories

Issued by Sandia National Laboratories, operated for the United States Department of Energy by Sandia Corporation.

Available to DOE and DOE contractors from
Office of Scientific and Technical Information
P.O. Box 62
Oak Ridge, TN 37831

Prices available from (615) 576-8401, FTS 626-8401

Available to the public from
National Technical Information Service
U.S. Department of Commerce
5285 Port Royal Rd
Springfield, VA 22161

NTIS price codes
Printed copy: A03
Microfiche copy: A01

SAND97-2214
Unlimited Release
Printed September 1997

Distribution
Category UC-701

ULTRA-HIGH-SPEED STUDIES OF SHOCK PHENOMENA IN A MINIATURIZED SYSTEM: A PRELIMINARY EVALUATION

Wayne M. Trott and Kenneth L. Erickson
Energetic and Multiphase Processes Department
Sandia National Laboratories
P. O. Box 5800
Albuquerque, New Mexico 87185-0834

Abstract

A laboratory-scale experimental test system for small-scale studies of shock phenomena has been assembled. This system uses a variety of miniature test platforms in which shock loading is provided by laser-driven flyer impact. Acceptor materials include thin-film explosives and high-density metal foils. Optical access is provided for high-speed optical diagnostics such as optically recording velocity interferometry and single-pulse Raman spectroscopy. The experimental assembly for Raman studies features a common laser source for both flyer generation and excitation of Raman scattering (to achieve high timing precision) and a detection scheme that uses the coupling fiber for the excitation source to collect with high efficiency backscattered Raman light. Preliminary system evaluation experiments indicate that detailed particle velocity studies of the dynamic material properties of high-density metals under short-pulse, high-strain-rate loading can be performed in a miniaturized test configuration. Single-pulse Raman studies on shock compressed thin film explosives also appear feasible if the thickness and grain structure of these films can be tailored to enhance the Raman scattering signal sufficiently. Possible improvements in the experimental design and a number of likely applications of these techniques are also discussed.

Acknowledgments

The excellent technical assistance of Jaime N. Castañeda is gratefully acknowledged. Flyer target materials were skillfully prepared by Catharine Sifford of the Thin Film, Vacuum & Brazing Department 1471 at Sandia National Laboratories.

Preface

This work was supported by Laboratory Directed Research and Development (LDRD) funding. The Appendix lists reporting information required by that funding source.

Contents

Figures

Figures (continued)

I. INTRODUCTION

Shocks produce an unusual realm of pressure and temperature, generated on a short time scale, that can induce a wide variety of physical and chemical changes in materials. These changes (and their underlying processes) provide a very rich area of inquiry and potential discovery of ongoing relevance to many Sandia National Laboratories programs, including weapon component design and evaluation, surety assessment, and advanced materials development. The pursuit of predictive understanding in this field (as well as its associated applications) requires a continuing investment in state-of-the-art experimental methods for real-time studies.

A viable experimental system for real-time examination of shock-induced physical and chemical changes in materials must combine techniques for well-controlled and well-characterized shock loading with suitable high-speed diagnostic methods. To approach optimal shock loading conditions, a large gas-gun driver is often used to generate high-speed plate impact in an analytically tractable (e.g., planar) geometry. Multi-stage guns are required to achieve impact velocities substantially greater than 2 km-s^{-1}. Studies involving complex test systems of this type are necessarily expensive and difficult to perform either rapidly or in large number. In general, these devices are not well suited to study shock-induced processes that occur with very short (i.e, nanosecond) time scales. Moreover, these large-scale systems are impractical for investigation of rare, expensive, or highly toxic materials.

Several alternative methods for high-amplitude shock loading on a small scale have been considered including electric exploding foil accelerators,[1] a light-ion-beam driver for flyer plate acceleration,[2] and direct irradiation of the target material with a high-intensity pulsed laser.[3] A recent approach adopted by several research groups involves radiation-induced shock generation in a hohlraum configuration.[4-6] Each of these methods offers advantages but is also subject to various significant limitations. For example, electric foil accelerators are unable to launch high-impedance metal flyers. In the direct laser irradiation technique, extensive tailoring of the laser temporal and spatial profile is required to avoid the production of ill-conditioned shock waves. The light-ion-beam and radiation drivers involve expensive test systems that generally do not permit rapid "turn around."

In this report, we describe preliminary efforts to develop, evaluate and use a unique, laboratory-scale capability for detailed examination of material response to well-controlled, short-duration shocks. This system combines [1] well-characterized techniques for nearly planar shock compression using laser-driven flyer plates, [2] thin-film or foil sample materials, and [3] high-speed, real-time optical diagnostics including optically recording velocity interferometry and single-pulse Raman spectroscopy. Experiments are performed with a variety of miniature test platforms that are designed for precisely timed optical access to the target material. In addition to providing a safe and relatively inexpensive alternative to many experiments performed using gas-gun drivers, this capability is designed to allow previously inaccessible regimes of shock states and chemical reactivity to be probed in detail. In particular, this concept represents a unique opportunity to study shock-induced thermomechanical and chemical processes that occur with extremely short (~1-5 ns) characteristic time scales--e.g., shock initiation of certain high explosives (such as fine-grain HNS and PETN) that can undergo transition to detonation under these conditions.

This project was initiated with the support of Laboratory Directed Research and Development (LDRD) funds received mid-year in FY96 and was assigned to the Phenomenological Modeling and Engineering Simulation Investment Area. In a review conducted a few months later, the Investment Area Team decided that the project fell outside the defined scope of this group and it was not recommended for continuation in FY97. Much of the short available time for this effort was devoted to apparatus design and assembly. As a result, the evaluation of the experimental concept summarized in this report is both preliminary and cursory; however, we include numerous recommendations for further exploration and application.

II. EXPERIMENTAL

A. Laser Drive Concept

The experimental system achieves nearly planar shock compression on a small scale (<1-mm diameter) using laser-driven flyer plates. Laser-launched aluminum flyers can easily achieve impact velocities exceeding 3 km-s^{-1}, resulting in shock pressures of several hundred kilobars in many materials. Shock durations, on the other hand, are only ~10 ns or less. Enabling techniques in this set-up include [1] the use of a laser source having a short coherence length (broad linewidth), [2] multimode, step-index optical tapers and fibers to couple the high-intensity optical radiation to the flyer target, and [3] composite flyer materials containing a thin, insulating barrier (e.g, Al_2O_3) to mitigate the deleterious effects of deep thermal diffusion. Properly configured, the laser driver and optical transmission system can generate a uniform spatial intensity profile at the target plane, promoting very nearly planar launch conditions with precisely variable impact velocities and accurate (~1 ns) timing[7-9]. A detailed description of the drive system components is given below.

B. Miniature Test Platforms

While the concept described in this report is applicable to a broad range of problems, we have focused on the feasibility of examining shock compression states and rapid chemical reactions in energetic materials. Test platforms designed for this task seek to achieve synergistic application of established techniques for thin-film energetic material preparation and high-speed optical diagnostics in combination with laser-driven flyer impact. One platform consists of a miniature fixture shown schematically in Fig. 1. This assembly contains the output faces (separated by a known distance) of two optical fibers. One fiber face is coated with the flyer target material and the second face is coated with a thin-film (~10 μm, appropriate to the time scale for well-characterized shock loading) sample of energetic material. The flyer impact velocity is controlled by varying the laser fluence reaching the fiber output face, the flyer target thickness, and the thickness of the spacer that defines the "flight distance" of the impactor. The second fiber is used to carry the excitation source for single-pulse Raman spectroscopy as well as the backreflected Raman scattering signal from the shock compressed sample. This diagnostic provides a molecular level probe of the response of the parent species to shock loading and may also allow transient species and final products of chemical reactions to be identified, if sufficient sensitivity can be achieved. Miniaturized hardware (including polished optical fiber substrates for the energetic material thin films) for this test platform was designed and fabricated.

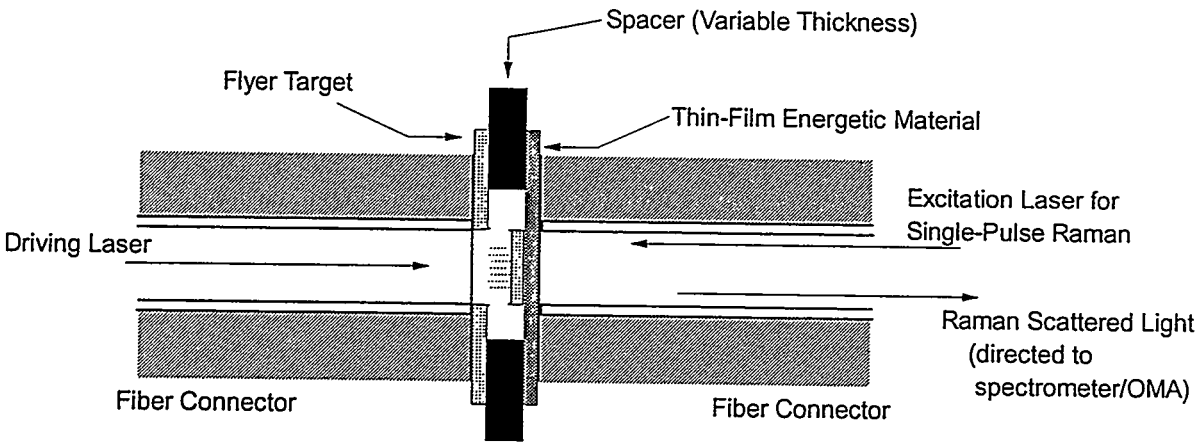

Figure 1. Schematic diagram of miniature test platform for single-pulse Raman studies of thin-film energetic materials under flyer impact.

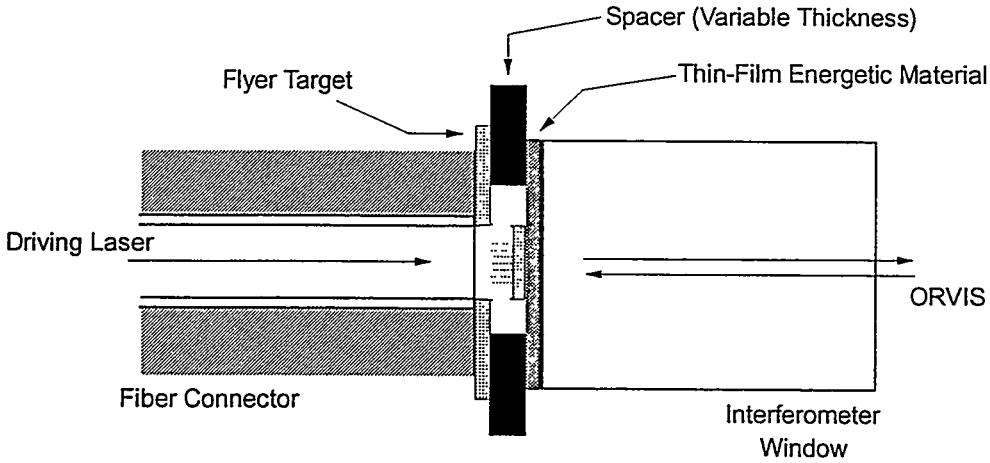

Figure 2. Schematic diagram of miniature test platform for particle velocity measurements of the response of thin-film energetic materials using an optically recording velocity interferometer system.

Complementary information about [1] the shock state of the unreacted energetic material or [2] global reaction progress (at sufficiently high shock pressure) can be obtained from high resolution particle velocity measurements. Figure 2 shows a schematic representation of a miniature fixture prepared for comparison of thin film shock properties with the known response of bulk energetic material. In this design, the flyer impacts a window prepared with a very thin (~50 nm) coating of reflecting material (e.g., aluminum) and a "top" layer of the thin film energetic material. An optically recording velocity interferometer system (ORVIS)[10] is used to determine the resulting particle velocity history at the interface. Many available window materials such as fused silica, sapphire, LiF and BaF_2 have been characterized for use in velocity interferometry. Optical access must be provided for the focused beam of the interferometer source laser (an Ar^+ continuous wave laser operated at 514.5 nm, ~1 W single line) as well as for the light reflected from the interface. The use of the very thin intermediate reflecting coating is a well-established technique for enhancing the reflected light signal without measurably perturbing the shock interaction at the interface. For films prepared with densities, grain sizes, etc. that are equivalent to well-characterized bulk material (see discussion on sample characterization in Section IIIA), the measured particle velocities can be directly compared to the known bulk response. This comparison allows changes at the molecular level (observed with spectroscopic methods) to be correlated with the applied shock pressure as a function of flyer impact velocity.

As the preceding discussion suggests, it would be desirable in many cases to tailor the energetic film deposition process to generate samples with properties closely matching interesting bulk materials (e.g., pressings of fine-particle HNS or PETN used in slapper initiation applications). On the other hand, the thin film explosives obtained under different deposition conditions may prove to be very interesting materials as well. Recent innovations in line-imaging velocity interferometry[11-13] may facilitate miniature scale equation-of-state measurements on these uncharacterized samples. A test platform designed for this task (not fabricated in the present work) is shown in Fig. 3. The step profile on the window face is employed in preparing two known thicknesses of sample. Shock propagation through the stepped sample allows both shock velocity and particle velocity to be measured with a line-imaging interferometer. A series of tests wherein these two quantities are determined can be used in conjunction with the Rankine-Hugoniot mass, momentum and energy jump conditions to derive a complete Hugoniot curve. In an alternative approach, the thin film energetic material could be deposited over the flyer target for use in "reverse impact" experiments on a regular interferometer window.

A different area addressed by this work involves the response of high-density metals to shock loading in a short-pulse, high-strain-rate ($>10^7$ s^{-1}) regime. A fixture designed for these experiments is shown schematically in Fig. 4. The response of a metal foil either in contact with an interferometer window or in a free surface configuration (as shown) can be examined in this setup. Miniature hardware for fixtures of this type was designed and fabricated. In these experiments, ORVIS can be used for high-speed measurements of shock attenuation, "pull-back" velocities of material going into tension, etc.

C. Sample Preparation

Flyer targets were prepared by physical vapor deposition on the output faces of 400-μm-diameter, step-index, multimode optical fibers. The primary target material was aluminum; however, a

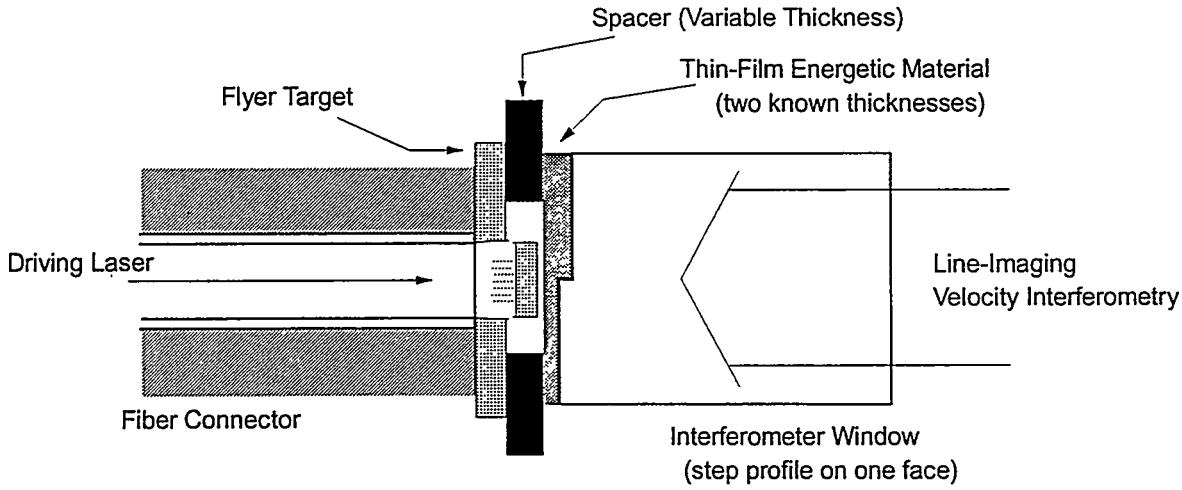

Figure 3. Schematic diagram of miniature test platform for equation of state measurements on thin-film energetic materials; simultaneous determination of shock velocity and particle velocity using a line-imaging velocity interferometer.

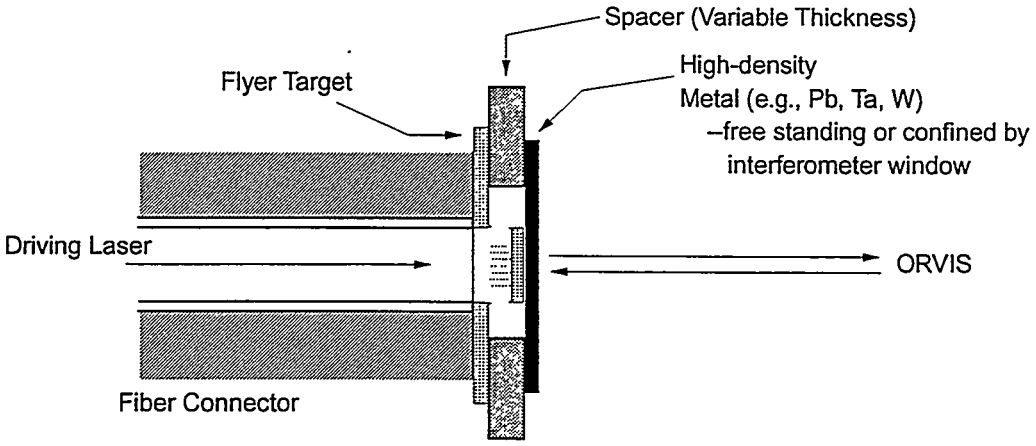

Figure 4. Schematic diagram of miniature test platform for particle velocity measurements of the response of a high-density metal foil upon flyer impact.

0.25-μm layer of Al_2O_3 was embedded in the film (at a location near the fiber output face) to retard thermal diffusion. This measure has proved to be somewhat effective in preventing heating, melting, etc. of the flyer material prior to impact.[9]

The thin film energetic material samples used in the present work were prepared by physical vapor deposition, a technique that provides reasonably precise control of film properties. This method can be used with any material that exerts sufficient vapor pressure (~10^{-5} - 10^{-3} Torr) at temperatures low enough to ensure negligible decomposition. Films (primarily TATB) were prepared on three different substrate types: [1] polished output faces at one end of six-inch-long optical fiber assemblies (for use in the test platform shown in Fig. 1); [2] 0.25-inch-diameter, 0.25-inch-thick optical windows (for use in the test platform shown in Fig. 2); and [3] thin sapphire discs (4.75-mm-diameter, 0.5-mm-thick). The samples prepared on the thin sapphire pieces were generated as part of a characterization scheme (cf. Section IIIA). The apparatus and basic procedures for the vapor deposition process have been described previously.[14] These procedures were followed with only minor modifications. In particular, special holders were fabricated to accommodate the different substrates in the deposition chamber.

The metal foils used in the test platform shown in Fig. 4 were obtained from commercial suppliers. A 0.25-inch-diameter punch was used to prepare discs of the appropriate size for the test fixture. Prior to assembly, burrs were clipped from the edge of the disc and the foil was pressed between two smooth surfaces to remove all coarse wrinkles.

D. Assembly for Single-Pulse Raman Spectroscopy

The experimental arrangement for single-pulse Raman spectroscopy studies is shown schematically in Fig. 5. To achieve the requisite timing precision for this application, it was desirable to have a common laser source for both flyer generation (the shock driver) and excitation of Raman scattering (the optical probe of the shock loaded material). The available laser best suited for this task was a pulsed Nd:YAG laser (1.064 μm, ~10-ns pulse duration) equipped with an in-line crystal for second harmonic generation at 532 nm. We used dichroic mirrors (labeled D1 and D2 in Fig. 5) to separate the frequency-doubled light from the unconverted fundamental radiation. This common source scheme ensures negligible "jitter" between the infrared and visible components. Facile and reproducible control of delay times between these components can be achieved through straightforward changes of propagation length in the corresponding optical transmission systems (see discussion below).

The 1.064-μm radiation was directed to the point of application with the aid of a coaxially aligned, continuous wave HeNe laser (λ = 632.8 nm). To align these sources, the Nd:YAG laser beam path was first determined by taking "burn spots" (using photographic film or commercial burn paper) at two locations: [1] in the near field, just behind an alignment iris (cf. Fig. 5) and [2] in the far field (ahead of the focusing lens labeled FL2 in Fig. 5). After aligning the iris opening to the burn record and then removing the burn paper or film, the HeNe laser was aligned to the iris opening and far-field burn spot via sequential adjustments of turning mirror, M2, and a second mirror, KM1, located on a removable kinematic mount. Using the HeNe laser as a visible guide, the infrared beam was focused onto the input end of an optical fiber taper (Fiberguide Industries, Stirling, NJ) in which the core diameter reduction (from 1000 μm to 400 μm) is achieved over a

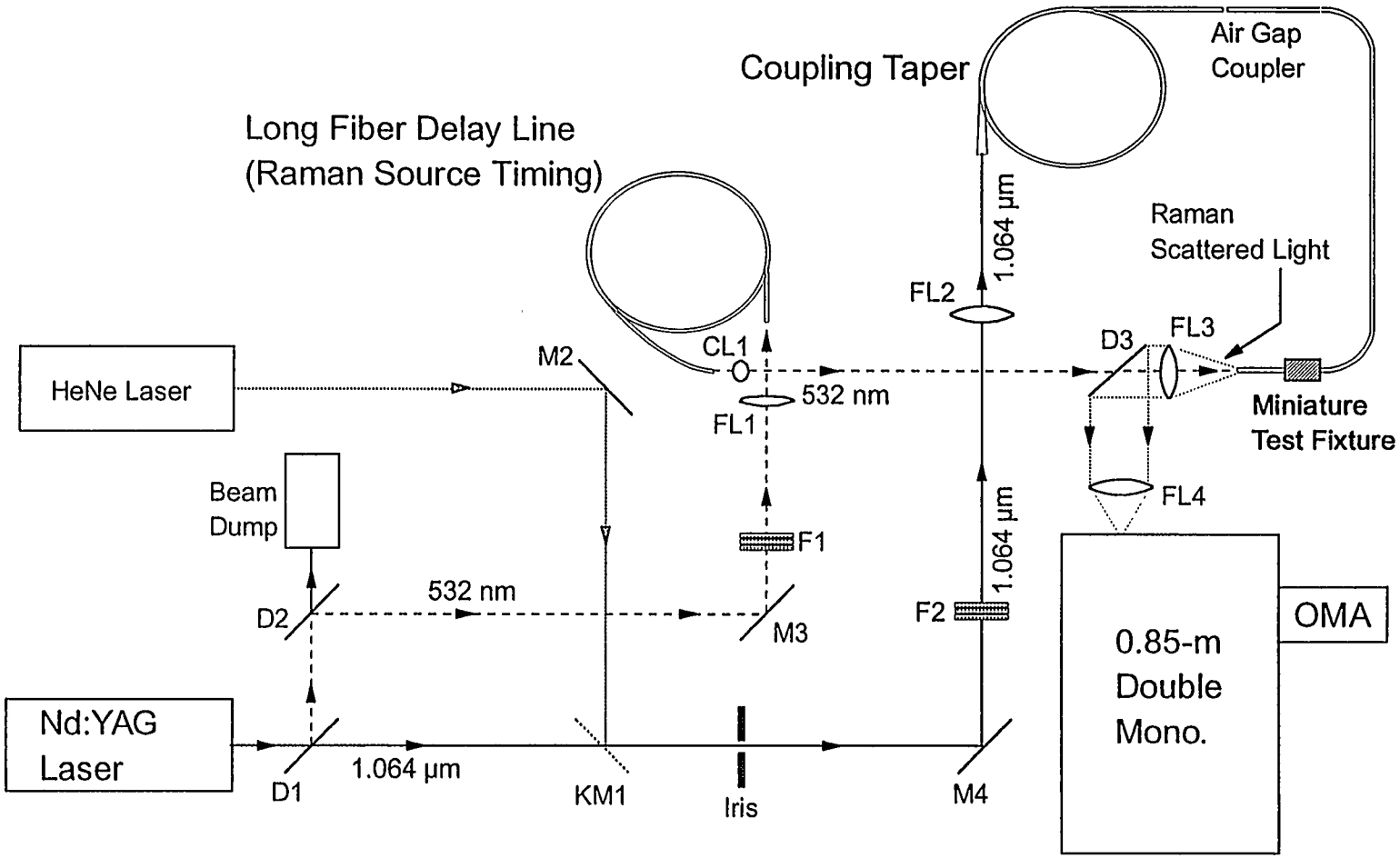

Figure 5. Schematic diagram of experimental arrangement for single-pulse Raman scattering studies. Numbered labels denote dichroic mirrors (D), mirrors (M), mirror on removable kinematic mount (KM), filters (F), focusing lenses (FL), collimating lens (CL)

length of approximately 1 meter. The input face of the taper was positioned slightly past the focus of lens FL2 so that the diverging beam just "filled" the 1000-μm core diameter. This coupling method was used to minimize the intensity of "hot spots" in the beam at the first air/fiber interface and also to provide for some homogenization of the laser intensity ahead of the core diameter reduction to 400 μm. The laser energy reaching the output end of the taper was coupled across a small air gap to the input face of a 1-meter-long polished fiber assembly (C Technologies, Inc., Cedar Knolls, NJ). The distal end of this assembly (coated with the flyer target material) was inserted into the miniature test fixture as illustrated in Fig. 1. Absorption-type neutral density filters (labeled F2 in Fig. 5) were used to adjust the laser output energy reaching the flyer target.

Active alignment of the frequency-doubled (532-nm) light was feasible with the Nd:YAG laser operating at 30 Hz and at relatively low power. In a manner similar to that described above, this light was focused onto the input end (300-μm core diameter) of a variable length optical fiber delay line. This component was designed to delay the Raman excitation source arrival time at the miniature test fixture (cf. Fig. 1) to compensate for the required flyer plate "flight time" across the gap distance defined by the spacer (~30-100 ns, depending on the flyer thickness, incident laser fluence, etc.). The optical propagation time delay, Δt, generated by this method is expressible in terms of absolute physical quantities; i.e., $\Delta t = ln/c$, where l represents the fiber length, c is the free-space velocity of light, and n is the refractive index of the material. For fused silica fiber, $n =$ 1.46071 at 532 nm. Hence, $\Delta t = 4.87$ ns per meter of fiber used in the delay line. Some consideration must also be given to the temporal dispersion in the fiber. The maximum delay time, t_d, of light propagating along off-axis paths in the fiber compared to on-axis rays is given by

$$t_d = \frac{l}{c} n_{co} \left(\frac{n_{co}}{n_{cl}} - 1 \right) \qquad (1)$$

where l and c are defined as before and n_{co} and n_{cl} are the refractive indices of the fiber core and cladding material, respectively.[15] For fiber with numerical aperture equal to 0.22 (as used in the present study), $t_d = 56$ ps/m. Since adequate delay times could be achieved with fiber lengths ≤ 20 meters, the timing uncertainty due to dispersion effects was ~1 ns or less, a relatively minor factor.

The temporally delayed 532-nm light exiting the fiber was collimated with a short focal length lens (labeled CL1 in Fig. 5) and transmitted through dichroic mirror D3. This light was focused by lens FL3 onto the input end of a six-inch-long fiber optic assembly. The distal end of this assembly (coated with the thin film energetic material) was installed in the test platform as shown in Fig. 1. Absorption-type neutral density filters (labeled F1 in Fig. 5) were also used in this beam path to adjust the intensity of the Raman excitation source.

In this experimental design, the fiber used to transmit the Raman excitation source to the thin film energetic material also serves as an efficient collector of Raman scattered light from the sample. This light exits the proximal face of the fiber optic assembly (in the direction opposite to that of the incoming laser pulse) and is nearly collimated by lens FL3 (cf. Fig. 5). The Raman signal is separated from backreflected and backscattered 532-nm light by reflecting it off the dichroic mirror (D3) and passing it through a 0.85-m double monochromator (Spex Model 1404). The dis-

persed spectrum is viewed by a silicon target vidicon coupled to a gateable proximity-focused channel intensifier tube (ITT/EOPD Model F4144), and the signal is processed by an optical multichannel analyzer (OMA). The detector is gated on by a voltage pulse that is triggered ahead of the excitation source pulse by using appropriate digital delay generators. In the present work, a 60-ns gate width was used to avoid any signal loss due to timing jitter and to provide some discrimination against background emission (e.g., long-lived sample fluorescence). This detection system allows 4-nm increments of the sample Raman spectrum to be viewed and recorded on a single shot. The spectral resolution is typically 0.05 nm (~1.5 cm^{-1} at 570 nm). Wavelength calibration was accomplished by using the known line positions in the uranium emission spectrum generated by a hollow-cathode discharge tube.[16]

Although the common source scheme used for both flyer generation and Raman excitation provides advantages in experiment timing, it requires some compromise of system performance. Ideally, a narrow linewidth source is desirable for Raman excitation (to minimize instrumental broadening of the Raman transitions) while a broad linewidth (short coherence length) is advantageous in minimizing the modal noise propagating down the drive system fibers, thereby providing a more uniform intensity distribution at the fiber/flyer target interface and, hence, a more planar flyer launch. The Nd:YAG laser used in the present work has a relatively long coherence length. In fact, the measured linewidth of the frequency-doubled (532-nm) light is 1.5 cm^{-1}, approximately equal to the spectrometer resolution. At the effective resolution provided by this arrangement, most Raman transitions can be observed with negligible broadening, even at high dispersion. On the other hand, the comparably narrow linewidth of the fundamental (1.064-μm) component may be expected to result in fairly severe fluctuations of the intensity distribution at the fiber/flyer target interface. To address this issue, we examined the spatial profile of light exiting the distal end of an uncoated 1-meter-long fiber assembly by generating a magnified image of the output face at the detector plane of a solid-state array camera. Intensity distributions were analyzed by a Multicam 2.0 beam profiling system (Big Sky Software, Bozeman, MT). Profiles along horizontal and vertical lines (scaled to the fiber core diameter) intersecting the centroid of the spatial distribution are shown in Fig. 6. The overall distribution (from edge to edge) is fairly flat; however, numerous high-frequency peak-to-valley fluctuations of 2-4 times in intensity are seen across the face of the fiber. At launch, these fluctuations may lead to nonplanar local segments in the flyer geometry and may also encourage the formation and growth of Rayleigh-Taylor instabilities.[17] A detailed examination of the evolving flyer geometry as a function of time is needed to address this concern.

We also obtained spatial profiles of the 532-nm light exiting the distal end of an uncoated fiber assembly. Typical horizontal and vertical line profiles are displayed in Fig. 7. Overall, the range of observed peak-to-valley fluctuations appears to be slightly less than that seen in the 1.064-μm light used as the flyer plate driver, possibly reflecting some damping of the modal noise in the long fiber delay line. A reasonably uniform Raman excitation source is useful in maximizing signal while avoiding optically induced damage in the sample.

E. Assembly for Particle Velocity Measurements

The experimental arrangement for particle velocity tests is shown schematically in Fig. 8. The driving laser used in these experiments was an actively Q-switched Nd:Glass oscillator (Laser-

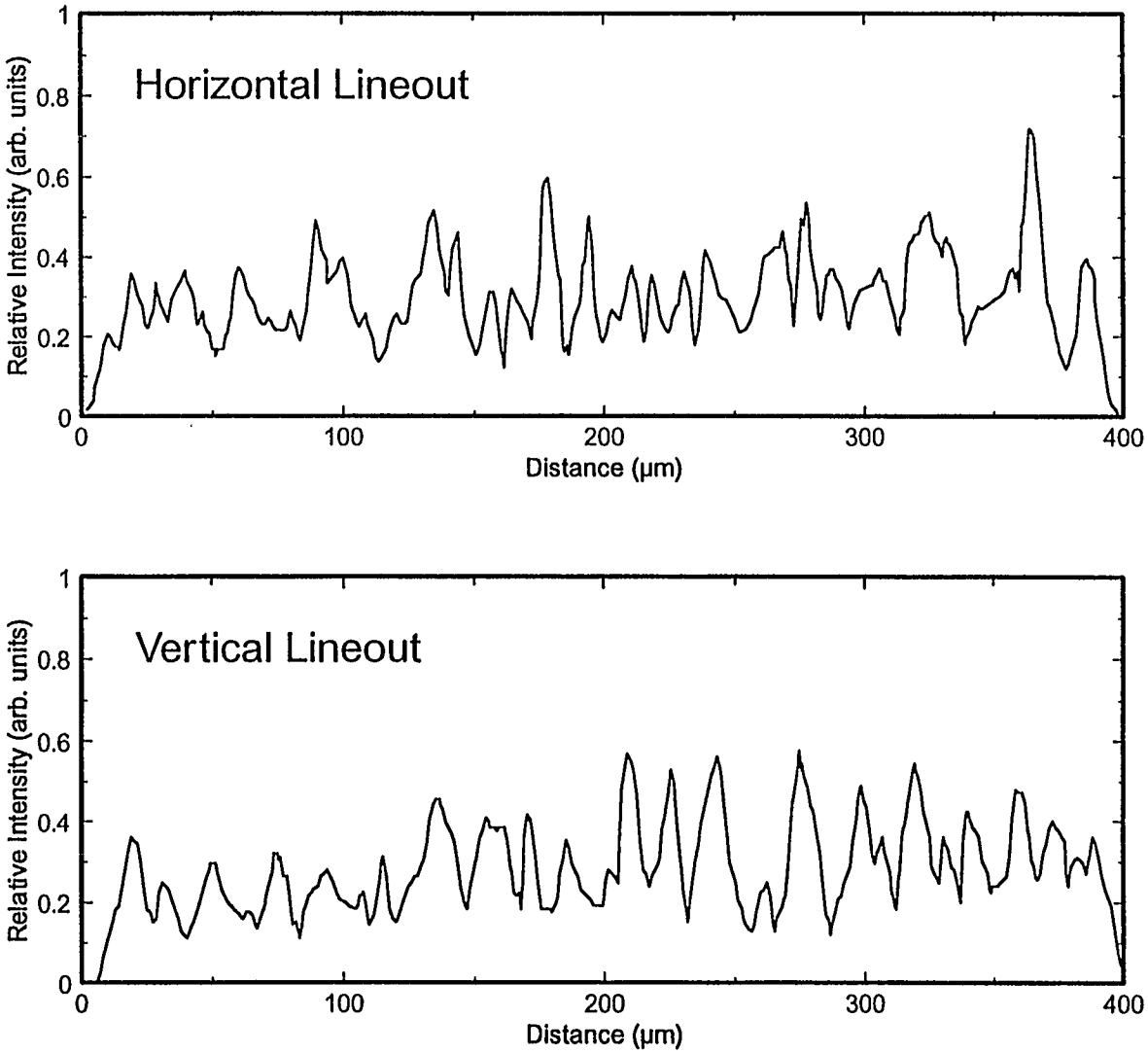

Figure 6. Spatial profile of the intensity of 1.064-μm light exiting a fiber assembly similar to that used for flyer launch. Horizontal and vertical line profiles intersecting the centroid of the spatial distribution are displayed.

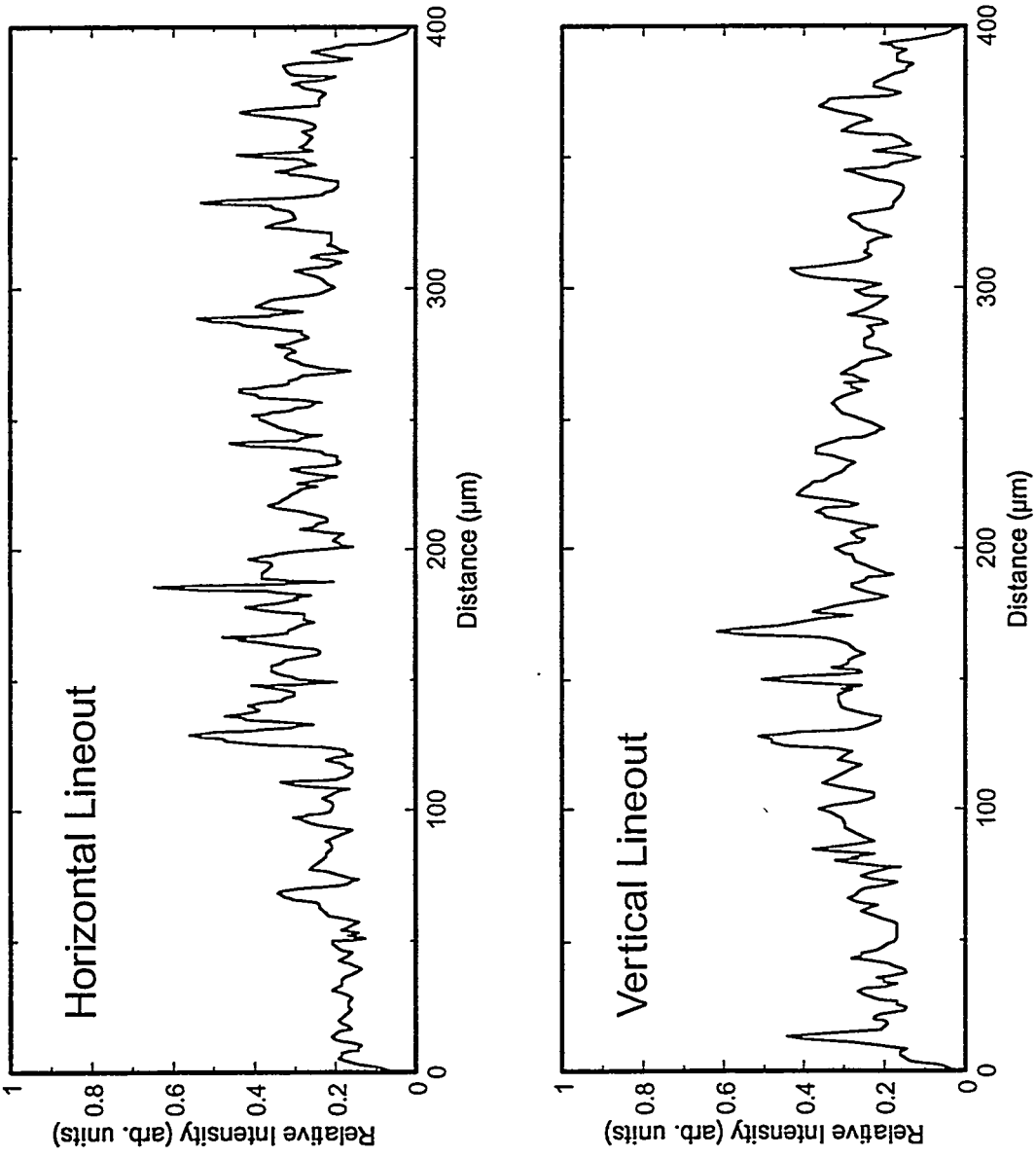

Figure 7. Spatial profile of the intensity of 532-nm light exiting a fiber assembly used to transmit the Raman excitation source. Horizontal and vertical line profiles intersecting the centroid of the spatial distribution are displayed.

metrics Model 9380). Various diagnostics were used to determine important characteristics of the light ($\lambda = 1.054$ μm) entering and exiting the coupling fibers. Incident or transmitted laser energy was measured by a calibrated power-energy meter. The temporal profile of the laser was routinely monitored using an appropriately filtered biplanar phototube coupled to fast oscilloscope (total time constant < 0.4 ns). The laser output was horizontally polarized and multimode. Coarse spectral analysis indicated that the output was also relatively broadband (~1.3 nm). Under these conditions, the observed spatial profile at the exit face of an optical fiber should contain relatively small intensity fluctuations due to modal noise propagation. This behavior was confirmed by measurements on uncoated fibers using a beam profiling analysis system.[9,18] By adjusting the flashlamp bank voltage, the laser pulse duration could be varied over the range 16-50 ns (FWHM). All measurements in the present work were performed with pulse durations near 18 ns.

Techniques for aligning the infrared Nd:Glass laser beam to the visible HeNe laser and for coupling laser energy into the optical fiber transmission system were essentially identical to those described in the previous section. The optical tapers and polished fiber optic assemblies were obtained from commercial suppliers (Fiberguide Industries and C Technologies, Inc., respectively). The distal end of the fiber optic assembly (coated with the flyer target material) was once again installed in one side of the appropriate miniature test fixture (cf. Fig. 4). Absorption-type neutral density filters (labeled F1 in Fig. 8) were used to regulate the optical energy reaching the flyer targets.

ORVIS was used to determine both flyer performance and velocity-time histories for the flyer-impacted samples. Key elements of the interferometer system are shown in Fig. 9. A detailed description of the interferometer characteristics and operation is given in Ref. 10. Briefly summarized, particle velocity is linearly proportional to interferometer fringe displacement using this technique. In the present work, the fringe motion was viewed by an electronic image-converter streak camera (Hadland Photonics, Ltd., IMACON 675) and recorded on an intensified CCD detector. Digital image analysis[19] was used to obtain accurate velocity-time records from the image data.

III. PRELIMINARY RESULTS AND RECOMMENDATIONS

A. Thin Film Energetic Material Sample Characterization

Previous work[14] using optical and scanning electron microscopy (SEM), x-ray diffraction, and transmission electron microscopy has shown that vapor deposited energetic material thin films are well crystallized and relatively uniform. Some additional characterization of the density, porosity, grain size distributions, etc. of the thin films is required for interpretation of shock compression experiments. This information is particularly vital to any attempt to correlate the response of shock-loaded thin films with the known behavior of well-characterized bulk materials. To address this need, we developed a sample characterization strategy that involves the following procedures: [1] film deposition on a low-mass substrate (i.e., the 0.5-mm-thick sapphire discs) to permit accurate measurement of the thin film mass using a microbalance with 0.1 μg sensitivity, [2] measurement of the flatness and uniformity of the thin film samples using an optical, non-contact profilometer, and [3] determination of grain sizes and void distributions from SEM images of sectioned samples. The microbalance and non-contact profilometry measure-

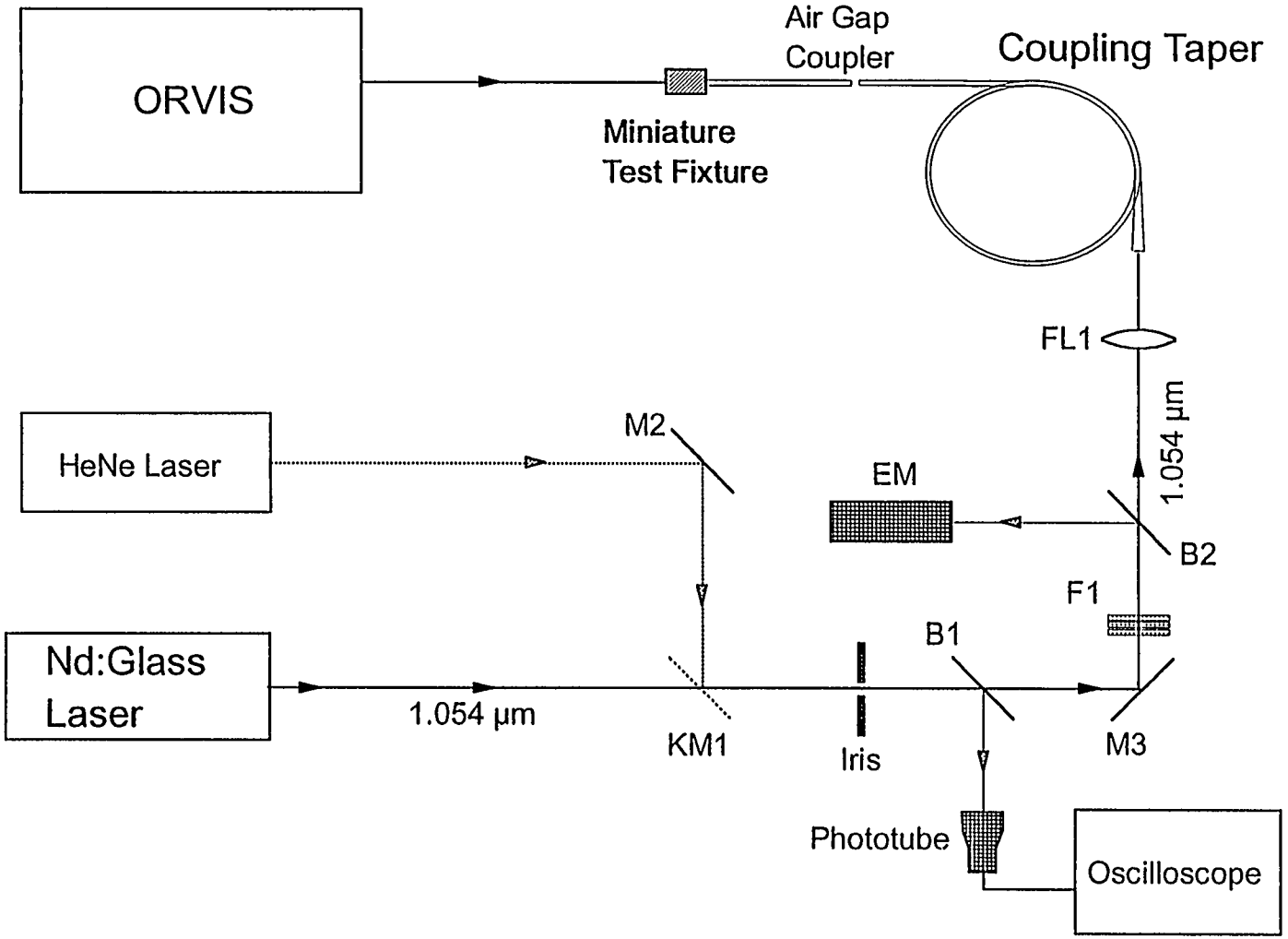

Figure 8. Schematic diagram of experimental arrangement for particle velocity measurements using an optically recording velocity interferometer system. Labels denote mirrors (M), mirror on removable kinematic mount (KM), filters (F), focusing lens (FL), beamsplitter (B), energy meter (EM).

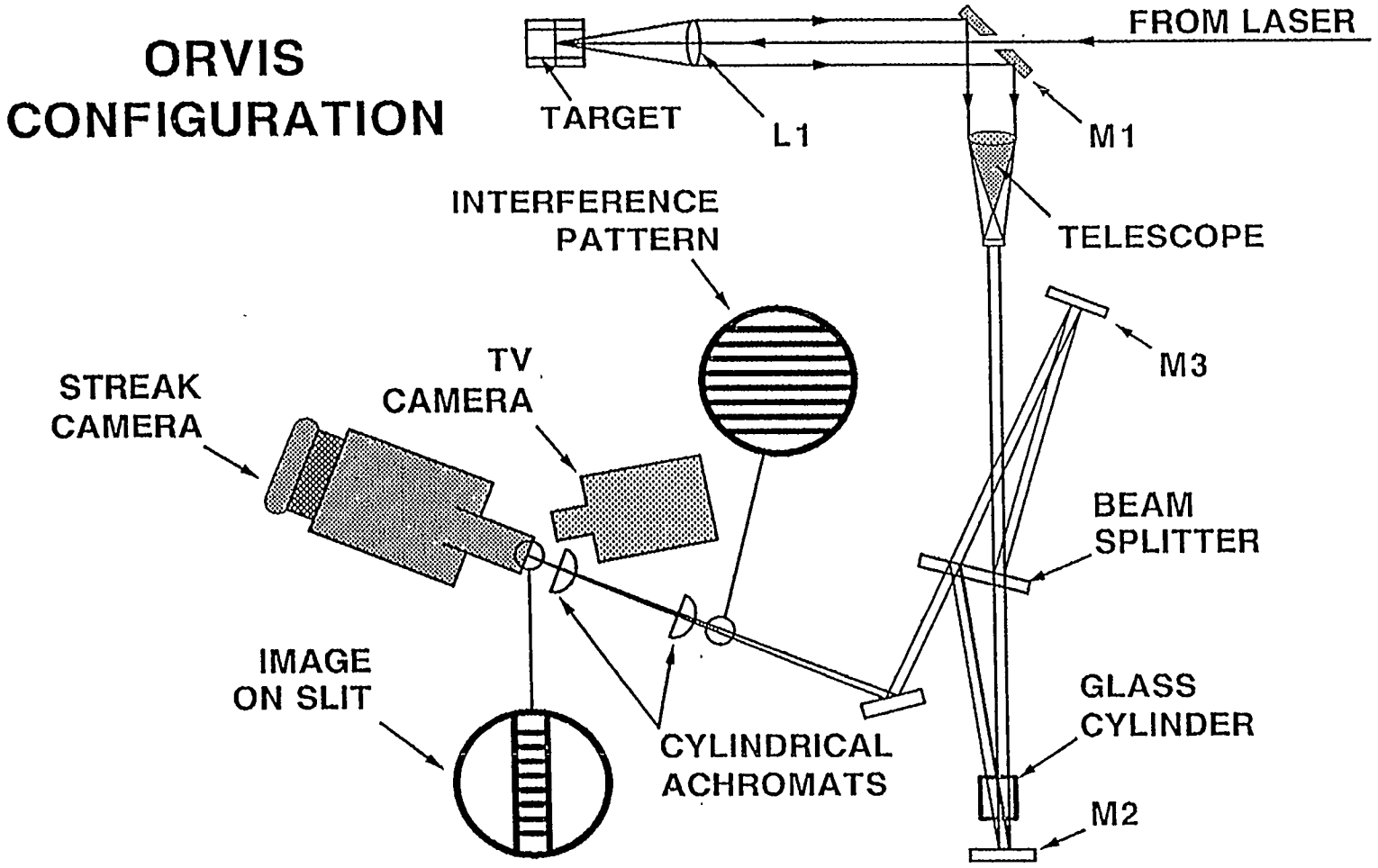

Figure 9. Schematic diagram showing principal elements of the optically recording velocity interferometer system (ORVIS).

ments can be performed directly on the 0.25-inch-diameter, 0.25-inch-thick interferometer windows as well. Optical microscopy and non-contact profilometry can be used to compare samples prepared on the polished fiber optic assemblies with those deposited on other substrates.

The TATB films prepared for this work were very uniform in appearance but somewhat thinner than expected (compared to previously observed deposition rates at a given temperature). A magnified image (obtained from a long-working-distance microscope) of a film prepared on one of the 0.5-mm-thick sapphire discs is displayed in Fig. 10. From microbalance measurements, the film thickness in this case was determined to be ~2 μm (assuming the theoretical maximum density). Under a microscope at high magnification, the grain structure was barely observable (i.e., very fine). The observed film properties were likely the result of the relatively low thermal mass of the substrate holders. With this condition, the sample/substrate was probably maintained at a somewhat higher temperature than those encountered in previous deposition runs.[14] A higher temperature undoubtedly promotes faster evaporation of the TATB, resulting in a relatively thin deposition; however, it should also lead to increased surface mobility, thereby generating a more uniform sample. Time did not permit us to examine these films with the optical profiler or to supply a sufficient quantity of sectioned films for SEM analysis.

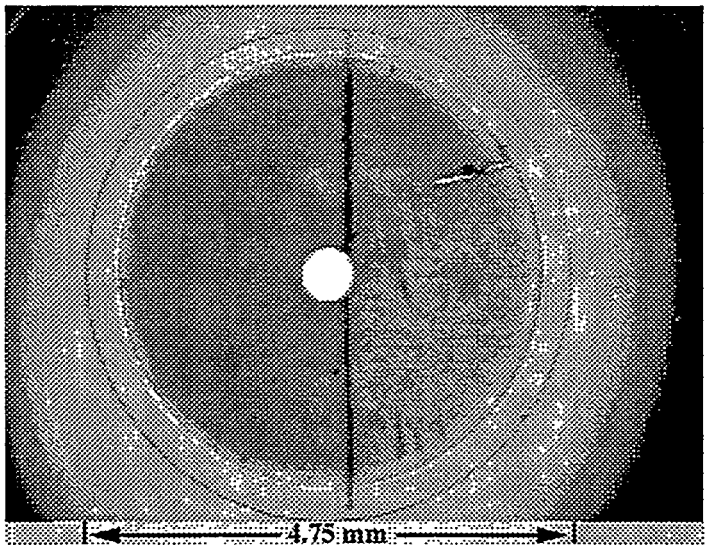

Figure 10. Long-working-distance microscope image of TATB thin film deposited on thin sapphire disc. Dark vertical line corresponds to scribe mark made to assist the sectioning of the disc/sample. Bright "circle" in the center results from a small opening in the disc. Also seen are a few scratches produced by handling.

B. Single-Pulse Raman Spectroscopy System Evaluation

For initial evaluation of the Raman spectroscopy setup, we transmitted the 532-nm light through the fiber delay line and coupled it into an uncoated, six-inch-long fiber optic assembly (cf. Fig. 5). Instead of installing the distal end of this assembly into the miniature test fixture, the output face was placed in close proximity to a pressed, granular pellet of a non-explosive substance; i.e., *trans*-stilbene. With this configuration, we were able to evaluate the collection efficiency of the fiber coupling scheme for Raman scattered light. Figure 11 displays a single-shot spectrum obtained using an excitation source energy of 1 mJ. The known[20] ring stretching (581.4 nm, 1594 cm^{-1}) and C=C stretching (582.9 nm, 1639 cm^{-1}) mode transitions in *trans*-stilbene are clearly seen. The required excitation source energy for this result is significantly lower than the 5-10 mJ typically employed in an earlier single-pulse Raman spectroscopy assembly.[21,22] The relatively efficient light collection efficiency in the present setup has the added benefit of minimizing the possibility of optically induced damage in the sample. In fact, we observed no discoloration or evidence of ablation in the *trans*-stilbene material.

We were not successful in obtaining useful Raman data from our initial run of TATB thin films deposited on the fiber optic assemblies. Visual inspection revealed that no optically induced damage occurred at the excitation source intensities used. Moreover, it was readily apparent that these fine-grain films were largely transparent to visible light. The light trapping that occurs in a heterogeneous sample with relatively large grains evidently plays a large role in enhancing the Raman signal intensity. The negative result obtained in our initial tests suggests that this application requires substantially thicker films (~10 μm or greater) with a coarser grain structure. Possible techniques for production of these films include extended deposition times or, with some materials, deposition from solution using either spin coating or an air brush applicator.

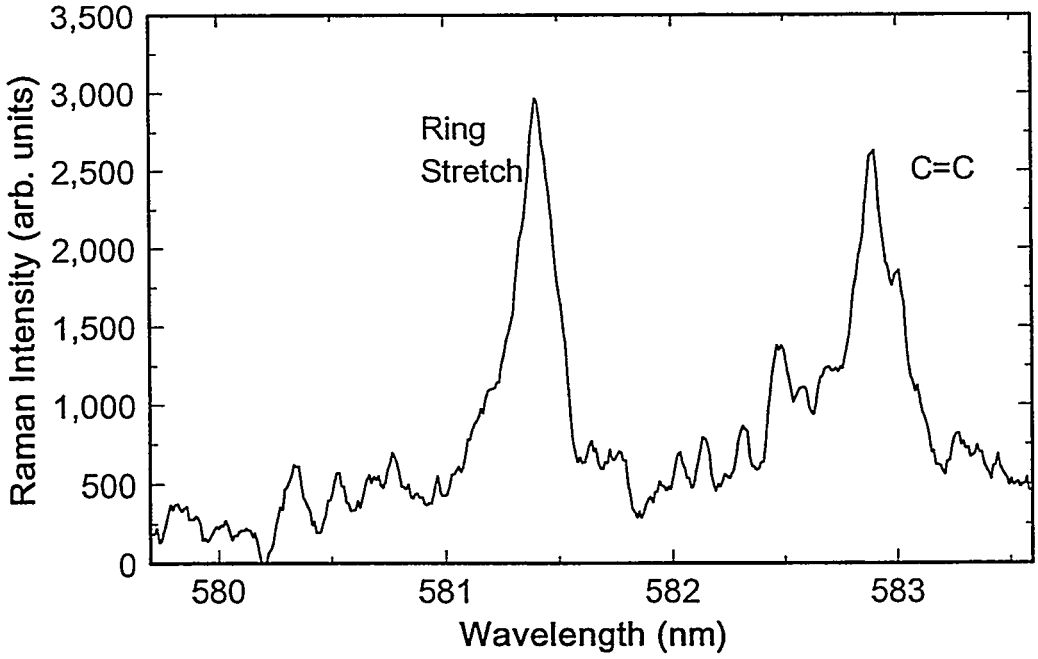

Figure 11. Single-pulse Raman spectrum from *trans*-stilbene. Fiber (400-μm diameter) used to transmit Raman excitation source and collect backscattered Raman signal.

C. Particle Velocity Measurements on High-Density Metal Foils

Evaluation experiments involving flyer impact on tantalum foils ($\rho = 16.65$ g-cm^{-3}) have been performed. These tests utilized the test platform configuration shown in Fig. 4 with velocity interferometry measurements on the available free surface of the Ta acceptor. The flyers were generated from a composite material containing a 0.25-μm-thick layer of Al_2O_3 embedded in aluminum. The total thickness of the composite material was 18 μm.

Figure 12 displays the velocity-time behavior of an 18-μm flyer for a particular drive condition: 400-μm fiber core diameter, 30 mJ incident energy, 18 ns pulse duration. Also shown is the calculated displacement vs. time. Repeated experiments at a fixed drive condition have demonstrated that shot-to-shot variations in flyer performance are quite small (2-3% or less). For a given "flight distance," the expected impact conditions can be derived from the velocity and displacement curves. With a 0.003" (76.2 μm) separation between flyer target and acceptor, impact should occur ~60 ns after the onset of flyer motion. The predicted impact velocity is ~1.7 km-s^{-1}.

The predicted shock interaction can be obtained graphically using the known Hugoniot curves[23] for Al and Ta, as illustrated in Fig. 13. Impact of pure Al at the relatively modest velocity of 1.7 km-s^{-1} should produce a high-amplitude (25 GPa) shock in the tantalum and introduce particle motion at a velocity of ~0.38 km-s^{-1} in the acceptor. Approximately twice this velocity should be recorded at the free surface.

The results of an impact experiment on a 12.5-μm-thick foil of tantalum are shown in Fig. 14. The maximum particle velocity measured by ORVIS is consistent with the predicted shock interaction. After the initial peak, a rapid "pull back" in the free surface velocity is observed. This behavior corresponds to the characteristic signature of a material going into tension. Tension states in the material are created from the interaction of rarefaction waves emanating from the target free surface and from the impactor. With appropriate choices of impactor and acceptor thickness, the tension state geometry can be tailored to generate a spall plane in the center of the acceptor. A series of experiments with an optimized geometry can be used to investigate the spall strength of the acceptor material. The preliminary data obtained here demonstrate that quantitative measurements of dynamic material properties can be obtained in a short-pulse, high-strain-rate regime and at the small scales of our miniature test platform. Straightforward improvements are possible in the design of the impactor/acceptor geometry as well as in the temporal resolution of the interferometer (determined by the optical delay incorporated in this device), recording speed, etc.

D. Recommendations for Future Work

Initial evaluation of the experimental concept summarized in this report indicates that high-speed diagnostics coupled with appropriately designed small scale test platforms utilizing laser-driven flyer impact can be used to address a number of interesting problems in shock compression science. The preliminary results suggest several potential improvements in the experimental design as well as additional areas of inquiry. In the single-pulse Raman spectroscopy application, a need for thicker energetic material films with coarser grain structure is readily apparent. Promis-

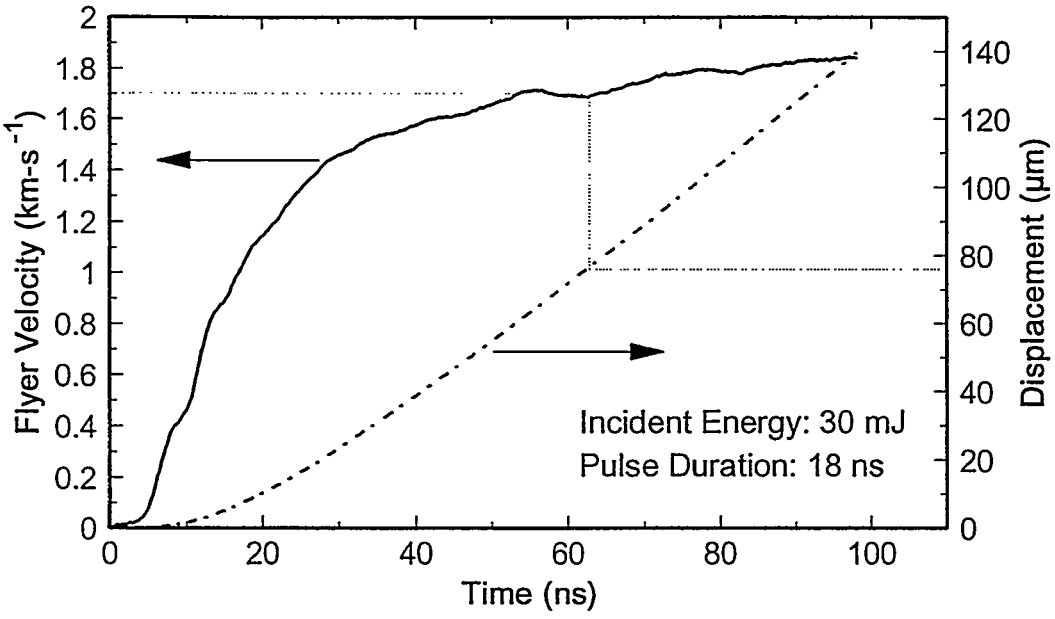

Figure 12. Velocity-time behavior of 18-μm composite flyer as determined by ORVIS. Also shown is the calculated displacement vs. time curve.

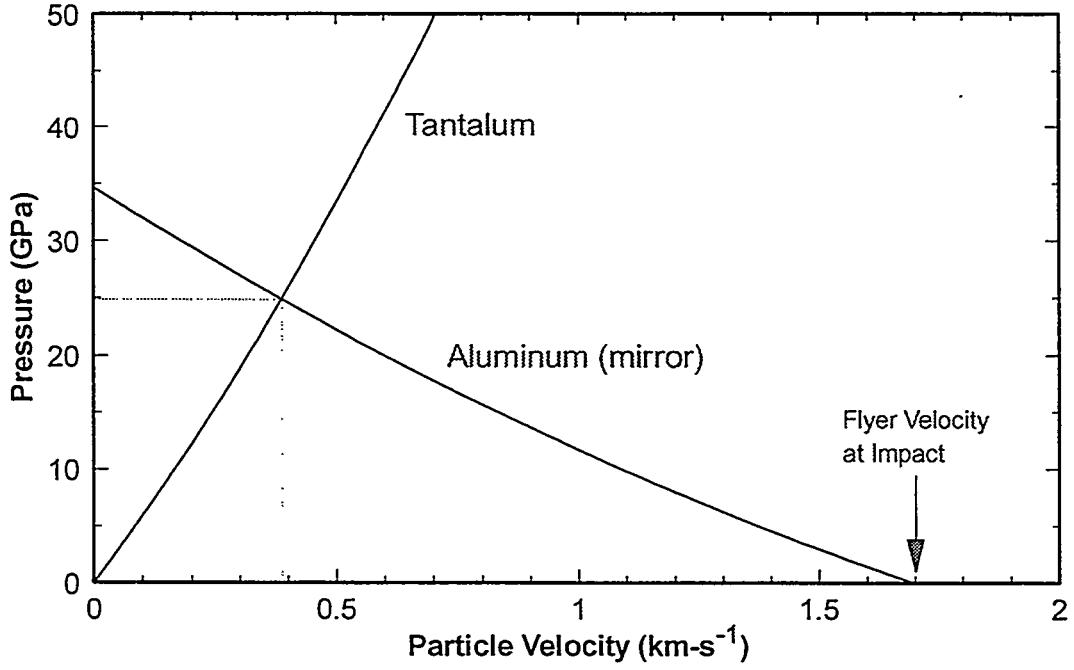

Figure 13. Graphical representation of shock interaction resulting from aluminum flyer impact (at 1.7 km-s^{-1}) on a tantalum acceptor.

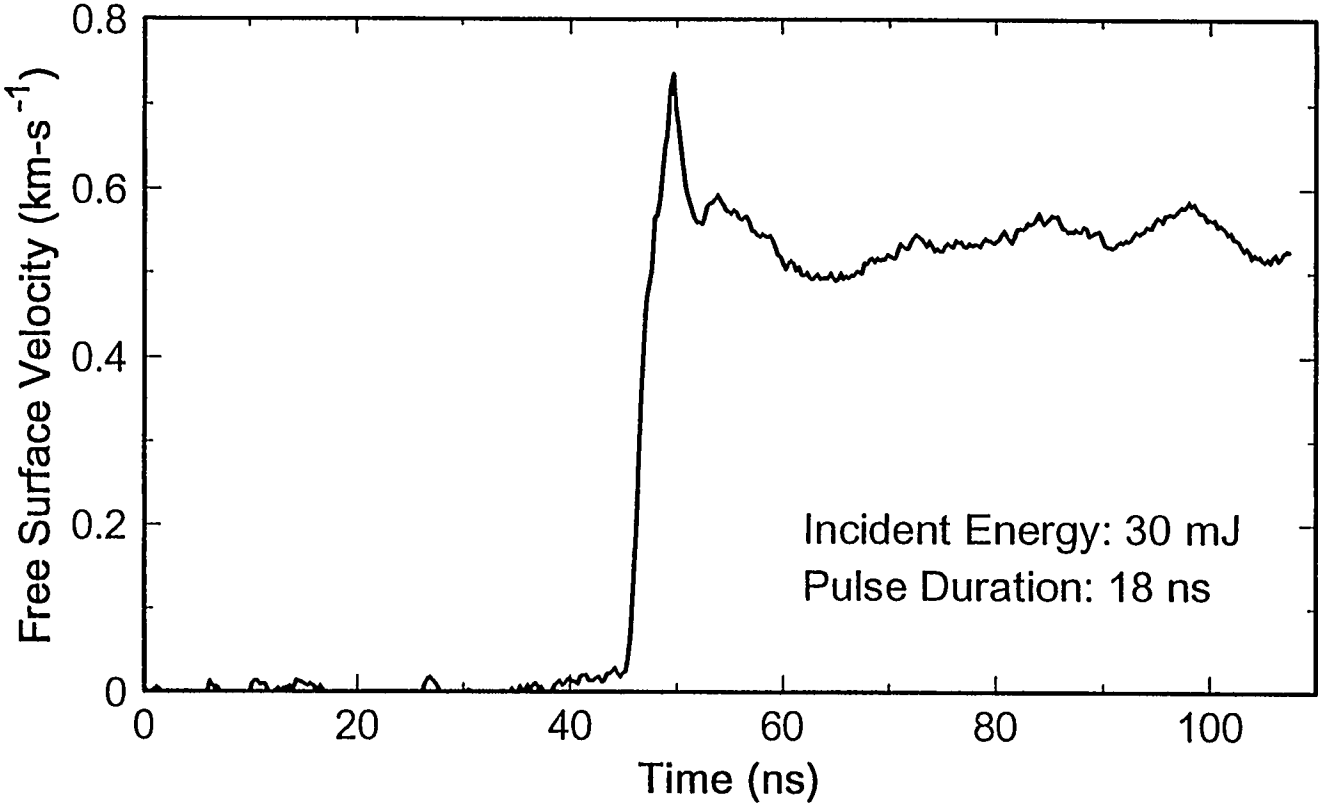

Figure 14. Free surface particle velocity vs. time (as determined by ORVIS) for 12.5-μm-thick tantalum acceptor impacted by composite flyer at 1.7 km-s^{-1} .

ing approaches to this problem include extended deposition times or, for some materials, the development of suitable techniques for deposition from solution. The characterization strategy outlined in Section IIIA needs to be fully implemented in order to define adequately the density, porosity, grain size distributions, etc. of the film samples. Considering the significant intensity fluctuations in the spatial profile of Nd:YAG laser light exiting a fiber, a reasonably complete characterization of the dynamic behavior of flyers launched with this driver needs to be performed. If adequate flyer planarity can not be achieved with this system, an alternative driver/ Raman excitation source needs to be developed. For investigation of high-density metals under the short-pulse, high-strain-rate conditions of flyer impact, experiments should be performed with an optimized impactor/acceptor geometry as well as with an optimized interferometer resolution and recording rate.

Long-term uses or extensions of this experimental capability might include the following:

[1] Short-duration shock compression studies of suitable TATB thin films using the single-pulse Raman probe with comparison of results to the known[21,22] response of bulk TATB under sustained shock loading--a plot showing the behavior of two Raman transitions under these conditions is reproduced in Fig. 15;

[2] Refinement of thin-film energetic material deposition processes to generate film densities and porosities that match properties of currently used bulk explosives as closely as possible--in particular, fine-grain formulations of explosives such as PETN or HNS that can undergo transition to detonation with extremely short time scales;

[3] Detailed tests of the response of PETN and HNS thin films to short-pulse shock loading (to promote and assist development of models of the initiation and transition-to-detonation behavior of these materials under these conditions)--high-speed velocity interferometry could be used to probe the equation of state of the unreacted explosive at previously inaccessible shock conditions and to measure time-to-reaction in the nanosecond regime; additional fundamental physical and chemical information might be obtained using the Raman probe;

[4] Evaluation of the response of energetic material thin films exhibiting significantly different morphologies than those occurring in bulk materials;

[5] Evaluation of strategies to extend the maximum available velocity of laser-generated flyers (presently ~4 km-s^{-1}) to the hypervelocity regime (>7 km-s^{-1}); factors contributing to flyer "failure" at elevated drive conditions include rapid diffusion of heat from the hot, driving plasma (leading to flyer melt and vaporization) and rapidly developing Rayleigh-Taylor instabilities--possible approaches to achieve acceptable mechanical integrity and higher velocities include the use of different composite flyer target materials and flyer generation with a broadband laser driver (to minimize instabilities driven by variations in the laser intensity at the fiber/flyer interface); as illustrated in Fig. 16, an extended velocity range would enable impact studies on high-density materials (such as lead) at shock pressures well in excess of 100 GPa;

[6] Detailed measurements of the dynamic material properties of a high-density metal foil (e.g., Ta or Pb) at high-strain-rate (>10^7 s^{-1}) conditions using ORVIS; results from a full test series would provide an important test for existing equation-of-state and dynamic material models in the short-pulse, high-strain-rate regime.

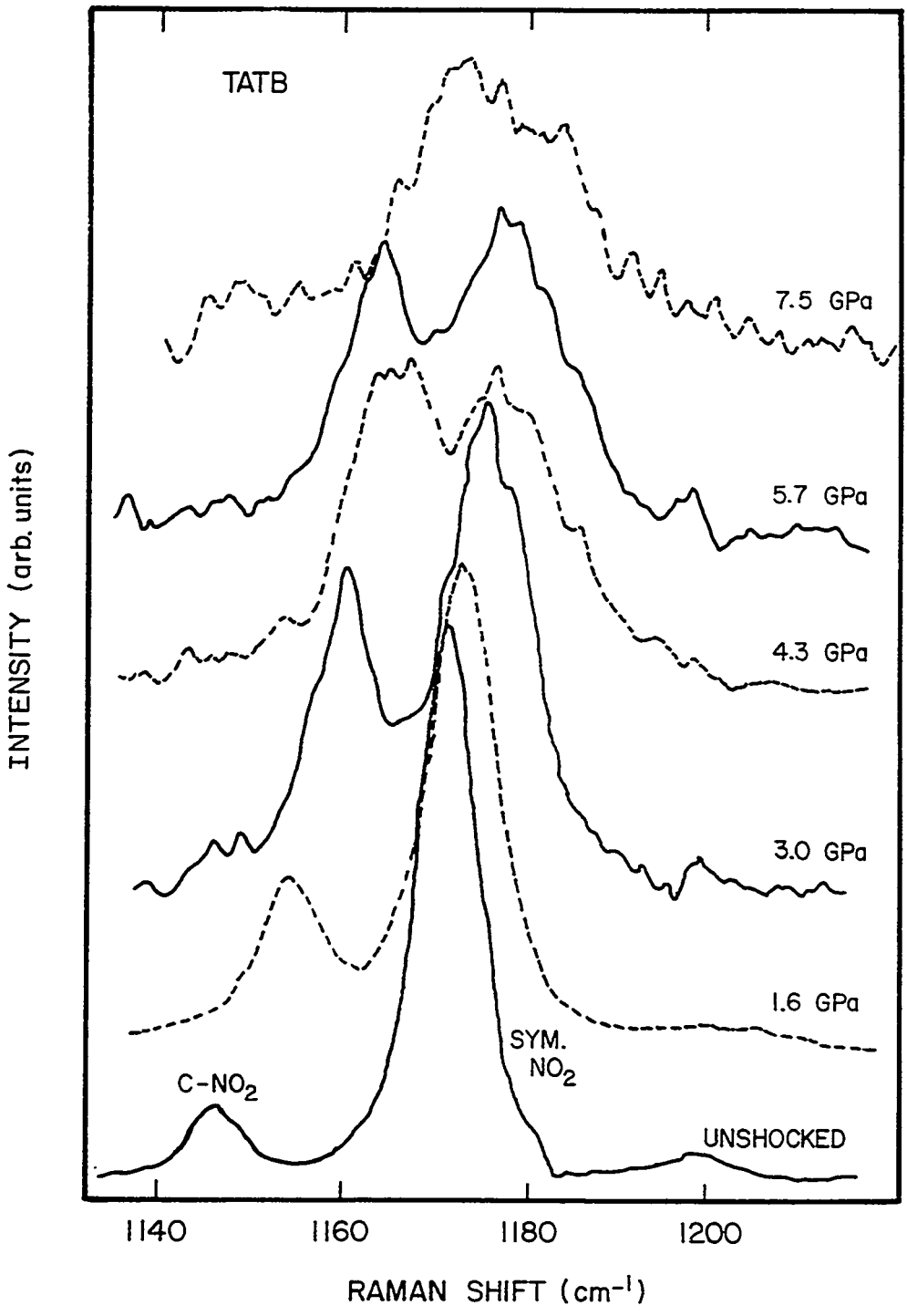

Figure 15. Response of two Raman transitions in TATB to sustained shock loading generated by a gas-gun driver (reproduced from Ref. 22)

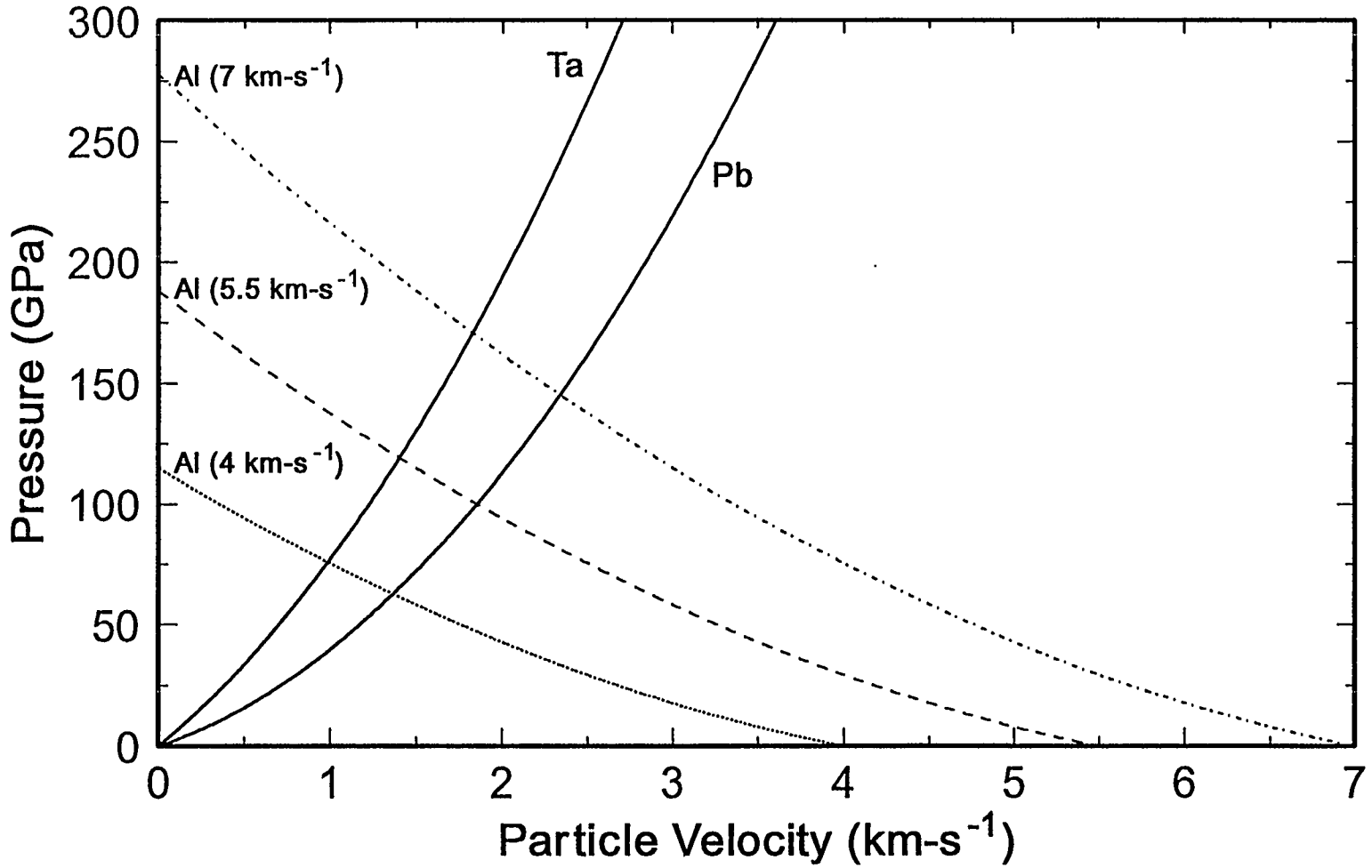

Figure 16. Graphical representation of shock interactions resulting from high-velocity aluminum flyer impacts on tantalum or lead acceptors (Hugoniot data from Ref. 23).

IV. CLOSURE

We have assembled a laboratory-scale experimental test system for shock compression studies utilizing a variety of miniature test platforms. The experimental capability combines [1] well-characterized techniques for short-duration, nearly planar shock compression using laser-driven flyer impactors, [2] thin-film or foil sample materials, and [3] high-speed optical diagnostics such as ORVIS and single-pulse Raman spectroscopy. Notable features of the experimental assembly developed for Raman studies include a common source for both flyer generation and excitation of Raman scattering (to achieve high timing precision via optical delays only) and a detection scheme that uses the coupling fiber for the excitation source to collect backscattered Raman light. Single-pulse Raman spectra with high signal-to-noise at high dispersion were obtained from a pressed, granular material at excitation source energies $\leq$ 1 mJ (sufficiently low to avoid optically induced damage in the sample). This result represents a significant improvement in collection efficiency compared to a previously developed single-pulse Raman spectroscopy system. Raman studies on shock loaded energetic material thin films appear feasible if the thickness and grain structure in these films can be tailored to increase the Raman scattering signal sufficiently. Preliminary particle velocity measurements of flyer impact on a high-density metal (e.g., Ta) acceptor indicate that detailed studies of dynamic material properties under short-pulse, high-strain-rate loading can be performed in a miniaturized system. Finally, we have identified several areas for improvement in the experimental design and suggested a number of interesting research problems that could benefit from this capability.

REFERENCES

1. R. Lee, J. Osher, H. Chau, M. Gerassimenko, G. Pomykal and R. Speer, *Int. J. Impact Engng.* **14**, 451 (1993).
2. H. Bachmann, K. Baumung, G. I. Kanel, H. U. Karow, V. Licht, D. Rusch, J. Singer and O. Stoltz, "Target Experiments with Light-Ion Beams at KALIF," 9th International Conference on High-Power Particle Beams, Paper #PB-43, Washington, DC, May 1992.
3. S. Eliezer, I. Gilath, and T. Bar-Noy, *J. Appl. Phys.* **67**, 715 (1990).
4. B. Faral, M. Koenig, J. M. Boudenne, D. Batani, A. Benuzzi, S. Bossi, M. Temporal, S. Atzeni, Th. Löwer, "EOS Impedance Matching Experiments at High Pressure with Smoothed Laser Beam," in *Shock Compression of Condensed Matter--1995*, S. C. Schmidt and W. C. Tao, eds., AIP Press, New York, 1996, pp. 943-946.
5. S. D. Rothman, A. M. Evans and N. J. Freeman, "Copper Shock Hugoniot Experiments Using High Power Lasers," in *Shock Compression of Condensed Matter--1995*, S. C. Schmidt and W. C. Tao, eds., AIP Press, New York, 1996, pp. 77-80.
6. C. H. Konrad, W. M. Trott, C. A. Hall, J. S. Lash, R. J. Dukart, D. L. Hanson, R. E. Olson, G. A. Chandler, K. J. Fleming, L. C. Chhabildas, T. G. Trucano and J. R. Asay, "Use of Z-Pinch Sources for High-Pressure Shock Wave Experiments," in *Shock Compression of Condensed Matter--1997*, S. C. Schmidt, D. P. Dandekar and J. W. Forbes, eds. (to be published).
7. R. J. Lawrence and W. M. Trott, *Int. J. Impact Engng.* **14**, 439 (1993).
8. W. M. Trott, "Studies of Laser-Driven Flyer Acceleration Using Optical Fiber Coupling," in *Shock Compression of Condensed Matter--1991*, S. C. Schmidt, R. D. Dick, J. W. Forbes and D. G. Tasker, eds., Elsevier, New York, 1992, pp. 829-832.

9. W. M. Trott, "Investigation of the Dynamic Behavior of Laser-Driven Flyers," in *High-Pressure Science and Technology--1993*, S. C. Schmidt, J. W. Shaner, G. A. Samara and M. Ross, eds., AIP Press, New York, 1994, pp. 1655-1658.
10. D. D. Bloomquist and S. A. Sheffield, *J. Appl. Phys.* **54**, 1717 (1983).
11. W. F. Hemsing, A. R. Mathews, R. H. Warnes, and G. R. Whittemore, "VISAR: Line-imaging Interferometer," in *SPIE Proceedings No. 1346*, San Diego, CA, 1990, pp. 133-140.
12. K. Baumung, J. Singer, S. V. Razorenov, and A. V. Utkin, "Hydrodynamic Proton Beam-Target Interaction Experiments Using an Improved Line-imaging Velocimeter," in *Shock Compression of Condensed Matter--1995*, S. C. Schmidt and W. C. Tao, eds., AIP Press, New York, 1996, pp. 1015-1018.
13. W. M. Trott and J. R. Asay, "Investigation of Microscale Shock Phenomena Using a Line-imaging Optically Recording Velocity Interferometer System," in *Shock Compression of Condensed Matter--1997*, S. C. Schmidt, D. P. Dandekar and J. W. Forbes, eds. (to be published).
14. K. L. Erickson, R. D. Skocypec, W. M. Trott and A. M. Renlund, "Development of Thin-Film Samples for Examining Condensed-Phase Chemical Mechanisms Affecting Combustion of Energetic Materials, in *Proceedings of the 15th International Pyrotechnics Seminar*, hosted by IIT Research Institute, Boulder, CO, 1990, pp. 239-260.
15. A. W. Snyder and J. D. Love, *Optical Waveguide Theory*, Chapman and Hall, New York, 1983, pp. 51-62.
16. B. A. Palmer, R. A. Keller, and R. Engleman, Jr., *An Atlas of Uranium Emission Intensities in a Hollow Cathode Discharge*, Los Alamos National Laboratory Report; LA-8251-MS, July 1980.
17. A. M. Frank and W. M. Trott, "Investigation of Thin Laser-Driven Flyer Plates Using Streak Imaging and Stop Motion Microphotography," in *Shock Compression of Condensed Matter--1995*, S. C. Schmidt and W. C. Tao, eds., AIP Press, New York, 1996, pp. 1209-1212.
18. W. M. Trott and K. D. Meeks, *J. Appl. Phys.* **67**, 3297 (1990).
19. G. A. Fisk, G. A. Mastin and S. A. Sheffield, *J. Appl. Phys.* **60**, 2266 (1986).
20. Z. Meic and H. Güsten, *Spectrochimica Acta* **34A**, 101 (1978).
21. W. M. Trott and A. M. Renlund, *J. Phys. Chem.* **92**, 5921 (1988).
22. W. M. Trott and A. M. Renlund, "Pulsed-Laser-Excited Raman Spectra of Shock-Compressed Triaminotrinitrobenzene," in *Proc. Ninth Symposium (International) on Detonation*, Portland, OR, 1989, pp. 153-161.
23. S. P. Marsh, ed., *LASL Shock Hugoniot Data*, U. California Press, Berkeley, CA, 1980.

APPENDIX

Required Reportable Information
Laboratory Directed Research and Development

FY96 Mid-year LDRD Project: Ultra-High-Speed Studies of Shock Phenomena in a Miniaturized System

Publications and presentations: none

Invention disclosures: none

Patents: none

Copyrights: none

Employee recruitment: none

Student involvement: none

Distribution:

1	MS-0188	C. E. Meyers, 4523
5	MS-0834	W. M. Trott, 9112
5	MS-0834	K. L. Erickson, 9112
1	MS-0834	A. C. Ratzel, 9112
1	MS-9018	Central Technical Files, 8940-2
5	MS-0899	Technical Library, 4916
2	MS-0619	Review & Approval Desk. 12690 For DOE/OSTI